

On the Four-Dimensional Formulation of Dimensionally Regulated Amplitudes

Raffaele A. Fazio,¹ Pierpaolo Mastrolia,^{2,3} Edoardo Mirabella,² and William J. Torres Bobadilla^{1,3}

¹*Departamento de Física, Universidad Nacional de Colombia, Ciudad Universitaria, Bogotá, D.C. Colombia*

²*Max-Planck-Institut für Physik, Föhringer Ring 6, 80805 München, Germany*

³*Dipartimento di Fisica e Astronomia, Università di Padova, and INFN*

Sezione di Padova, via Marzolo 8, 35131 Padova, Italy

(Dated: August 21, 2018)

We propose a pure four-dimensional formulation (FDF) of the d -dimensional regularization of one-loop scattering amplitudes. In our formulation particles propagating inside the loop are represented by massive internal states regulating the divergences. The latter obey Feynman rules containing multiplicative selection rules which automatically account for the effects of the extra-dimensional regulating terms of the amplitude. The equivalence between the FDF and the Four Dimensional Helicity scheme is discussed. We present explicit representations of the polarization and helicity states of the four-dimensional particles propagating in the loop. They allow for a complete, four-dimensional, unitarity-based construction of d -dimensional amplitudes. Generalized unitarity within the FDF does not require any higher-dimensional extension of the Clifford and the spinor algebra. Finally we show how the FDF allows for the recursive construction of d -dimensional one-loop integrands, generalizing the four-dimensional open-loop approach.

I. INTRODUCTION

The recent development of novel methods for computing one-loop scattering amplitudes has been highly stimulated by a deeper understanding of their multi-channel factorization properties in special kinematic conditions enforced by on-shellness [1, 2] and generalized unitarity [3, 4], strengthened by the complementary classification of the mathematical structures present in the residues at the singular points [5–7].

The unitarity-based methods, reviewed in [8–15], use two general properties of scattering amplitudes such as analyticity and unitarity. The former grants that the amplitudes can be reconstructed from their singularity-structure while the latter grants that the residues at the singular points factorize into products of simpler amplitudes.

Integrand-reduction methods [5, 16], instead, allow one to decompose the integrands of scattering amplitudes into multi-particle poles, and the multi-particle residues are expressed in terms of *irreducible scalar products* formed by the loop momenta and either external momenta or polarization vectors constructed out of them. The polynomial structure of the multi-particle residues is a *qualitative* information that turns into a *quantitative* algorithm for decomposing arbitrary amplitudes in terms of Master Integrals (MIs) by polynomial fitting at the integrand level. In this context the on-shell conditions have been used as a computational tool reducing the complexity of the algorithm. A more intimate connection among the idea of reduction under the integral sign and analyticity and unitarity has been pointed out recently. Using basic principles of algebraic geometry, Refs. [6, 7, 17–19] have shown that the structure of the multi-particle poles is determined by the zeros of the denominators involved in the corresponding multiple cut. This new approach to integrand reduction methods allows for their systematization and for their all-loop extension.

Moreover, the proper understanding of the integrands of the amplitudes paved the way to the recent proposal of a four-dimensional renormalization scheme, which allows one to recognize and subtract UV-divergent contributions already at the integrand level [20–22].

Dimensionally-regulated amplitudes are constituted by terms containing (poly)logarithms, also called cut-constructible terms, and rational terms. The former may be obtained by the discontinuity structure of integrals over the four-dimensional loop momentum. The latter ones, instead, escape any four-dimensional detectability and require to cope with integrations including also the $(d - 4)$ components of the loop momentum.

Within generalized-unitarity methods both terms can be in principle obtained by performing d -dimensional generalized cuts [23–28]. In this context, the issue of addressing factorization in conjunction with regularization clearly emerges, since d -dimensional unitarity requires to work with tree-level amplitudes involving external particles in arbitrary, non-integer dimensions. Polarization states, dimensionality of the on-shell momenta, and the completeness relations for the particles wavefunctions have to be consistently handled since the number of spin eigenstates depends on the space-time dimension. Therefore, in many cases generalized unitarity in arbitrary non-integer dimensions is avoided and cut-constructible and rational terms are obtained in separate steps. The former are computed by performing four-dimensional generalized cuts in the un-regularized amplitudes. If possible the rational terms are obtained by using special properties of the amplitude under consideration, like the supersymmetric decomposition [29, 30].

Within integrand reduction methods, different approaches are available, according to the strategies adopted for the determination of cut-constructible and rational terms.

In some algorithms, the computation of the two ingredients proceeds in two steps: the cut-constructible

part is obtained by reducing the un-regularized integrand while the rational one is computed by introducing new counterterm-like diagrams which depend on the model under consideration [31, 32].

Other methods, instead, aim at the combined determination of the two ingredients by reducing the dimensionally regulated integrand. Therefore the numerator of the integrand has to be generated and manipulated in d dimensions and acquires a dependence on $(d - 4)$ and on the square of the $(d - 4)$ -dimensional components of the loop momentum, μ^2 [27, 28, 33]. The multi-particle residues are finally determined by performing generalized cuts by setting d -dimensional massive particles on shell. This is equivalent to have on-shell four-dimensional states whose squared mass is shifted by μ^2 .

If the integrand at a generic multiple cut is obtained as a product of tree-level amplitudes, the issues related to factorization in presence of dimensional regularization have to be addressed. An interesting approach [27] uses the linear dependence of the amplitude on the space-time dimensionality to compute the d -dimensional amplitude. In particular the latter is obtained by interpolating the values of the one-loop amplitude in correspondence to two different integer values of the space-time. When fermions are involved, the space-time dimensions have to admit an explicit representation of the Clifford algebra [28]. More recently, this idea has been combined with the six-dimensional helicity formalism [34] for the analytic reconstruction of one-loop scattering amplitudes in QCD via generalized unitarity.

In this article, we propose a four dimensional formulation (FDF) of the d -dimensional regularization scheme which, at one loop, turns out to be equivalent to the four-dimensional helicity (FDH) scheme [24, 35, 36], and which allows for a purely four-dimensional regularization of the amplitudes. Within FDF, the states in the loop are described as four dimensional massive particles. The four-dimensional degrees of freedom of the gauge bosons are carried by *massive vector bosons* of mass μ and their $(d - 4)$ -dimensional ones by *real scalar particles* obeying a simple set of four-dimensional Feynman rules. A d -dimensional fermion of mass m is instead traded for a *tachyonic Dirac field* with mass $m + i\mu\gamma^5$. The d dimensional algebraic manipulations are replaced by four-dimensional ones complemented by a set of multiplicative selection rules. The latter are treated as an algebra describing internal symmetries.

Within integrand reduction methods, our regularization scheme allows for the simultaneous computation of both the cut-constructible and the rational terms by employing a purely four-dimensional formulation of the integrands. As a consequence, an explicit four-dimensional representation of generalized states propagating around the loop can be formulated. Therefore, a straightforward implementation of d -dimensional generalized unitarity within exactly four space-time dimensions can be realized, avoiding any higher-dimensional extension of ei-

ther the Dirac [27, 28] or the spinor algebra [37].

Another interesting consequence of our framework is the possibility to extend to d dimensions the recursive generation of the integrand from off-shell currents and open loops, now limited to four dimensions [38–40].

The paper is organized as follows. Section II is devoted to the description of our regularization method, while Section III describes how generalized unitarity method can be applied in presence of a FDF of one-loop amplitudes. Section IV shows the decomposition in terms of MIs of certain classes of $2 \rightarrow 2$ one-loop amplitudes. It is preliminary to Sections V, VI and VII, which collect the applications of generalized unitarity methods within the FDF. In particular they present results for representative helicity amplitudes of $gg \rightarrow gg$, $q\bar{q} \rightarrow gg$ with massless quarks, and $gg \rightarrow Hg$ in the heavy-top limit. Section VIII describes how the integrand of the FDF of one-loop amplitudes can be generated recursively within the open-loop approach.

II. FOUR-DIMENSIONAL FEYNMAN RULES

The FDH scheme [24, 35, 36] defines a d -dimensional vector space embedded in a larger d_s -dimensional space, $d_s \equiv (4 - 2\epsilon) > d > 4$. The scheme is determined by the following rules

- The loop momenta are considered to be d -dimensional. All observed external states are considered as four-dimensional. All unobserved internal states, *i.e.* virtual states in loops and intermediate states in trees, are treated as d_s -dimensional.
- Since $d_s > d > 4$, the scalar product of any d - or d_s -dimensional vector with a four-dimensional vector is a four-dimensional scalar product. Moreover any dot product between a d_s -dimensional tensor and a d -dimensional one is a d -dimensional dot product.
- The Lorentz and the Clifford algebra are performed in d_s dimensions, which has to be kept distinct from d . The matrix γ^5 is treated using the 't Hooft-Veltman prescription, *i.e.* γ^5 commutes with the Dirac matrices carrying -2ϵ indices.
- After the γ -matrix algebra has been performed, the limit $d_s \rightarrow 4$ has to be performed, keeping d fixed. The limit $d \rightarrow 4$ is taken at the very end.

In the following d_s -dimensional quantities are denoted by a bar. One can split the d_s -dimensional metric tensor as follows

$$\bar{g}^{\mu\nu} = g^{\mu\nu} + \tilde{g}^{\mu\nu}, \quad (1)$$

in terms of a four-dimensional tensor g and a -2ϵ -dimensional one, \tilde{g} , such that

$$\tilde{g}^{\mu\rho} g_{\rho\nu} = 0, \quad \tilde{g}^\mu{}_\mu = -2\epsilon \xrightarrow{d_s \rightarrow 4} 0, \quad g^\mu{}_\mu = 4, \quad (2)$$

The tensors g and \tilde{g} project a d_s -dimensional vector \bar{q} into the four-dimensional and the -2ϵ -dimensional subspaces respectively,

$$q^\mu \equiv g^\mu{}_\nu \bar{q}^\nu, \quad \tilde{q}^\mu \equiv \tilde{g}^\mu{}_\nu \bar{q}^\nu. \quad (3)$$

At one loop the only d -dimensional object is the loop momentum $\bar{\ell}$. The square of its -2ϵ dimensional component is defined as:

$$\tilde{\ell}^2 = \tilde{g}^{\mu\nu} \bar{\ell}_\mu \bar{\ell}_\nu \equiv -\mu^2. \quad (4)$$

The properties of the matrices $\tilde{\gamma}^\mu = \tilde{g}^\mu{}_\nu \bar{\gamma}^\nu$ can be obtained from Eq. (2)

$$[\tilde{\gamma}^\alpha, \gamma^5] = 0, \quad \{\tilde{\gamma}^\alpha, \gamma^\mu\} = 0, \quad (5a)$$

$$\{\tilde{\gamma}^\alpha, \tilde{\gamma}^\beta\} = 2\tilde{g}^{\alpha\beta}. \quad (5b)$$

We remark that the -2ϵ tensors can not have a four-dimensional representation. Indeed the metric tensor \tilde{g} is a tripotent matrix

$$\tilde{g}^{\mu\rho} \tilde{g}_{\rho\nu} \tilde{g}^{\nu\sigma} = \tilde{g}^{\mu\sigma}, \quad (6)$$

and its square is traceless

$$\tilde{g}^{\mu\rho} \tilde{g}_{\rho\mu} = \tilde{g}^\mu{}_\mu \xrightarrow{d_s \rightarrow 4} 0, \quad (7)$$

but in any integer-dimension space the square of any non-null tripotent matrix has an integer, positive trace [41]. Moreover the component $\tilde{\ell}$ of the loop momentum vanishes when contracted with the metric tensor g ,

$$\tilde{\ell}^\mu g_{\mu\nu} = \bar{\ell}_\rho \tilde{g}^{\rho\mu} g_{\mu\nu} = 0, \quad (8)$$

and in four dimensions the only four vector fulfilling (8) is the null one. Finally in four dimensions the only non-null matrices fulfilling the conditions (5a) are proportional to γ^5 , hence $\tilde{\gamma} \sim \gamma^5$. However the matrices $\tilde{\gamma}$ fulfill the Clifford algebra (5b), thus

$$\tilde{\gamma}^\mu \tilde{\gamma}_\mu \xrightarrow{d_s \rightarrow 4} 0, \quad \text{while} \quad \gamma^5 \gamma^5 = \mathbb{I}. \quad (9)$$

These arguments exclude any four-dimensional representation of the -2ϵ subspace. It is possible, however, to find such a representation by introducing additional rules, called in the following -2ϵ selection rules, (-2ϵ) -SRs. Indeed, as shown in Appendix A, the Clifford algebra (5b) is equivalent to

$$\dots \tilde{\gamma}^\alpha \dots \tilde{\gamma}_\alpha \dots = 0, \quad \tilde{\ell} \tilde{\ell} = -\mu^2. \quad (10)$$

Therefore any regularization scheme which is equivalent of FDH has to fulfill the conditions (2) – (5a), and (10). The orthogonality conditions (2) and (3) are fulfilled by splitting a d_s -dimensional gluon onto a four-dimensional one and a colored scalar, s_g , while the other conditions are fulfilled by performing the substitutions:

$$\tilde{g}^{\alpha\beta} \rightarrow G^{AB}, \quad \tilde{\ell}^\alpha \rightarrow i\mu Q^A, \quad \tilde{\gamma}^\alpha \rightarrow \gamma^5 \Gamma^A. \quad (11)$$

The -2ϵ -dimensional vectorial indices are thus traded for (-2ϵ) -SRs such that

$$\begin{aligned} G^{AB} G^{BC} &= G^{AC}, & G^{AA} &= 0, & G^{AB} &= G^{BA}, \\ \Gamma^A G^{AB} &= \Gamma^B, & \Gamma^A \Gamma^A &= 0, & Q^A \Gamma^A &= 1, \\ Q^A G^{AB} &= Q^B, & Q^A Q^A &= 1. \end{aligned} \quad (12)$$

The exclusion of the terms containing odd powers of μ completely defines the FDF, and allows one to build integrands which, upon integration, yield to the same result as in the FDH scheme.

The rules (12) constitute an abstract algebra which is similar to the algebras implementing internal symmetries. For instance, in a Feynman diagrammatic approach the (-2ϵ) -SRs can be handled as the color algebra and performed for each diagram once and for all. In each diagram, the indices of the (-2ϵ) -SRs are fully contracted and the outcome of their manipulation is either 0 or ± 1 . It is worth to remark that the replacement of $\tilde{\gamma}^\alpha$ with γ^5 takes care of the d_s -dimensional Clifford algebra automatically, thus we do not need to introduce any additional scalar particle for each fermion flavor. These particles and their interactions have been instead introduced in Ref. [42], where a method for the reconstruction of the μ^2 -dependent part of the numerator has been proposed.

To summarize, the QCD d -dimensional Feynman rules in the 't Hooft-Feynman gauge, collected in Ref. [43], may have the following four-dimensional formulation:

$$\text{gluon} \quad \begin{array}{c} \bullet \text{---} k \text{---} \bullet \\ a, \alpha \quad b, \beta \end{array} = -i \delta^{ab} \frac{g^{\alpha\beta}}{k^2 - \mu^2 + i0} \quad (13a)$$

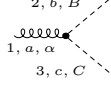
$$\text{ghost} \quad \begin{array}{c} \bullet \text{---} k \text{---} \bullet \\ a \quad b \end{array} = i \delta^{ab} \frac{1}{k^2 - \mu^2 + i0} \quad (13b)$$

$$\text{scalar} \quad \begin{array}{c} \bullet \text{---} k \text{---} \bullet \\ a, A \quad b, B \end{array} = -i \delta^{ab} \frac{G^{AB}}{k^2 - \mu^2 + i0}, \quad (13c)$$

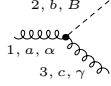
$$\text{fermion} \quad \begin{array}{c} \bullet \text{---} k \text{---} \bullet \\ i \quad j \end{array} = i \delta^{ij} \frac{\not{k} + i\mu\gamma^5 + m}{k^2 - m^2 - \mu^2 + i0}, \quad (13d)$$

$$\begin{array}{c} \begin{array}{c} 2, b, \beta \\ \bullet \text{---} k \text{---} \bullet \\ 1, a, \alpha \quad 3, c, \gamma \end{array} \end{array} = -g f^{abc} [(k_1 - k_2)^\gamma g^{\alpha\beta} + (k_2 - k_3)^\alpha g^{\beta\gamma} + (k_3 - k_1)^\beta g^{\gamma\alpha}], \quad (13e)$$

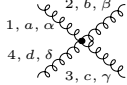
$$\begin{array}{c} \begin{array}{c} 2, b \\ \bullet \text{---} k \text{---} \bullet \\ 1, a, \alpha \quad 3, c \end{array} \end{array} = -g f^{abc} k_2^\alpha, \quad (13f)$$



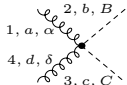
$$= -g f^{abc} (k_2 - k_3)^\alpha G^{BC}, \quad (13g)$$



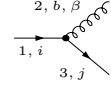
$$= \mp g f^{abc} (i\mu) g^{\gamma\alpha} Q^B, \quad (\tilde{k}_1 = 0, \quad \tilde{k}_3 = \pm \tilde{\ell}) \quad (13h)$$



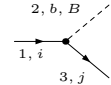
$$= -ig^2 \left[\begin{aligned} & f^{xad} f^{xbc} (g^{\alpha\beta} g^{\delta\gamma} - g^{\alpha\gamma} g^{\beta\delta}) \\ & + f^{xac} f^{xbd} (g^{\alpha\beta} g^{\delta\gamma} - g^{\alpha\delta} g^{\beta\gamma}) \\ & + f^{xab} f^{xdc} (g^{\alpha\delta} g^{\beta\gamma} - g^{\alpha\gamma} g^{\beta\delta}) \end{aligned} \right], \quad (13i)$$



$$= 2ig^2 g^{\alpha\delta} (f^{xab} f^{xcd} + f^{xac} f^{xbd}) G^{BC}, \quad (13j)$$



$$= -ig (t^b)_{ji} \gamma^\beta, \quad (13k)$$



$$= -ig (t^b)_{ji} \gamma^5 \Gamma^B. \quad (13l)$$

In the Feynman rules (13) all the momenta are incoming and the scalar particle s_g can circulate in the loop only. The terms μ^2 appearing in the the propagators (13a)–(13d) enter only if the corresponding momentum k is d -dimensional, *i.e.* only if the corresponding particle circulates in the loop. In the vertex (13h) the momentum k_1 is four-dimensional while the other two are d -dimensional. The possible combinations of the -2ϵ components of the momenta involved are

$$\{\tilde{k}_1, \tilde{k}_2, \tilde{k}_3\} = \{0, \mp \tilde{\ell}, \pm \tilde{\ell}\}. \quad (14)$$

The overall sign of the Feynman rule (13h) depends on which of the combinations (14) is present in the vertex.

The (-2ϵ) -SRs (12) and the Feynman rules (13) have been implemented in FEYNARTS [44] and FORM-CALC [45–47] and have been used to generate the numerators of the one-loop integrands of the processes

$$\begin{aligned} q\bar{q} &\rightarrow t\bar{t}, & gg &\rightarrow t\bar{t}, & t\bar{t} &\rightarrow t\bar{t}, \\ gg &\rightarrow gg, & q\bar{q} &\rightarrow t\bar{t}g, & gg &\rightarrow t\bar{t}g, \\ q\bar{q} &\rightarrow t\bar{t}q'q'. \end{aligned} \quad (15)$$

We have analytically checked that the numerators of the integrands obtained using FDF are equivalent to the corresponding ones obtained using the FDH scheme. In particular, we have verified that their difference is spurious,

i.e. it vanishes upon integration over the loop momentum.

Our prescriptions, Eq. (11), can be related to a five-dimensional theory characterized by $g^{55} = -1$, $\ell^5 = \mu$ and a 4×4 representation of the Clifford algebra, $\{\gamma^0, \dots, \gamma^3, i\gamma^5\}$. Regularization methods in five dimensions have been proposed as an alternative formulation of the Pauli-Villars regularization [48] or as regulators of massless pure Yang Mills theories at one loop [49]. Our method distinguishes itself by the presence of the (-2ϵ) -SRs, a crucial ingredient for the correct reconstruction of dimensionally-regularized amplitudes.

III. GENERALIZED UNITARITY

Generalized-unitarity methods in d dimensions require an explicit representation of the polarization vectors and the spinors of d -dimensional particles. The latter ones are essential ingredients for the construction of the tree-level amplitudes that are sewn along the generalized cuts. In this respect, the FDF scheme is suitable for the four-dimensional formulation of d -dimensional generalized unitarity. The main advantage of the FDF is that the four-dimensional expression of the propagators of the particles in the loop admits an explicit representation in terms of generalized spinors and polarization expressions, whose expression is collected below.

In the following discussion we will decompose a d -dimensional momentum $\bar{\ell}$ as follows

$$\bar{\ell} = \ell + \tilde{\ell}, \quad \bar{\ell}^2 = \ell^2 - \mu^2 = m^2, \quad (16)$$

while its four-dimensional component ℓ will be expressed as

$$\ell = \ell^b + \hat{q}_\ell, \quad \hat{q}_\ell \equiv \frac{m^2 + \mu^2}{2\ell \cdot q_\ell} q_\ell, \quad (17)$$

in terms of the two massless momenta ℓ^b and q_ℓ .

Spinors – The spinors of a d -dimensional fermion have to fulfill a completeness relation which reconstructs the numerator of the cut propagator,

$$\begin{aligned} & \sum_{\lambda=1}^{2^{(d_s-2)/2}} u_{\lambda,(d)}(\bar{\ell}) \bar{u}_{\lambda,(d)}(\bar{\ell}) = \bar{\ell} + m, \\ & \sum_{\lambda=1}^{2^{(d_s-2)/2}} v_{\lambda,(d)}(\bar{\ell}) \bar{v}_{\lambda,(d)}(\bar{\ell}) = \bar{\ell} - m. \end{aligned} \quad (18)$$

The substitutions (11) allow one to express Eq. (18) as follows:

$$\begin{aligned} & \sum_{\lambda=\pm} u_\lambda(\ell) \bar{u}_\lambda(\ell) = \ell + i\mu\gamma^5 + m, \\ & \sum_{\lambda=\pm} v_\lambda(\ell) \bar{v}_\lambda(\ell) = \ell + i\mu\gamma^5 - m. \end{aligned} \quad (19)$$

where p_i is the momentum of the particle i . In general, a massless four-point one-loop amplitude can be decomposed in terms MIs, as follows

$$A_4 = \frac{1}{(4\pi)^{2-\epsilon}} \left[c_{1|2|3|4;0} I_{1|2|3|4} + (c_{12|3|4;0} I_{12|3|4} + c_{1|2|3|4;0} I_{12|3|4} + c_{1|2|3|4;0} I_{12|3|4} + c_{1|2|3|4;0} I_{12|3|4}) \right. \\ \left. + (c_{12|3|4;0} I_{12|3|4} + c_{23|41;0} I_{23|41}) \right] + \mathcal{R}, \quad (32a)$$

$$\mathcal{R} = \frac{1}{(4\pi)^{2-\epsilon}} \left[c_{1|2|3|4;4} I_{1|2|3|4}[\mu^4] + (c_{12|3|4;2} I_{12|3|4}[\mu^2] + c_{1|2|3|4;2} I_{1|2|3|4}[\mu^2] + c_{1|23|4;2} I_{1|23|4}[\mu^2] + c_{2|3|41;2} I_{2|3|41}[\mu^2]) \right. \\ \left. + (c_{12|3|4;2} I_{12|3|4}[\mu^2] + c_{23|41;2} I_{23|41}[\mu^2]) \right]. \quad (32b)$$

We consider also the process involving three gluons, 1, 2, 3, and a Higgs boson, H ,

$$0 \rightarrow 1(p_1) 2(p_2) 3(p_3) H(p_H), \quad (33)$$

in the large top-mass limit [54, 55]. The one-loop amplitude for this process is decomposed as follows,

$$A_{4,H} = \frac{1}{(4\pi)^{2-\epsilon}} \left[(c_{1|2|3|H;0} I_{1|2|3|H} + c_{1|2|H|3;0} I_{1|2|H|3} + c_{1|H|2|3;0} I_{1|H|2|3} + (c_{12|3|H;0} I_{12|3|H} + c_{12|H|3;0} I_{12|H|3} + c_{1|23|H;0} I_{1|23|H} + c_{1|H|23;0} I_{1|H|23} + c_{2|H|31;0} I_{2|H|31} + c_{H|2|31;0} I_{H|2|31} + c_{1|2|3H;0} I_{1|2|3H} + c_{1|2H|3;0} I_{1|2H|3} + c_{1H|2|3;0} I_{1H|2|3}) \right. \\ \left. + (c_{12|3H;0} I_{12|3H} + c_{23|H1;0} I_{23|H1} + c_{H2|31;0} I_{H2|31}) + c_{123|H;0} I_{123|H} \right] + \mathcal{R}_H, \quad (34a)$$

$$\mathcal{R}_H = \frac{1}{(4\pi)^{2-\epsilon}} \left[(c_{1|2|3|H;4} I_{1|2|3|H}[\mu^4] + c_{1|2|H|3;4} I_{1|2|H|3}[\mu^4] + (c_{12|3|H;2} I_{12|3|H}[\mu^2] + c_{12|H|3;2} I_{12|H|3}[\mu^2] + c_{1|23|H;2} I_{1|23|H}[\mu^2] + c_{1|H|23;2} I_{1|H|23}[\mu^2] + c_{2|H|31;2} I_{2|H|31}[\mu^2] + c_{H|2|31;2} I_{H|2|31}[\mu^2] + c_{1|2|3H;2} I_{1|2|3H}[\mu^2] + c_{1|2H|3;2} I_{1|2H|3}[\mu^2] + c_{1H|2|3;2} I_{1H|2|3}[\mu^2]) \right. \\ \left. + (c_{12|3H;2} I_{12|3H}[\mu^2] + c_{23|H1;2} I_{23|H1}[\mu^2] + c_{H2|31;2} I_{H2|31}[\mu^2] + c_{123|H;2} I_{123|H}[\mu^2]) \right], \quad (34b)$$

The expressions for the MIs appearing in Eq. (32) and (34) are given in Appendix D.

In Eq. (32) and (34), the contribution generating the rational terms have been collected in \mathcal{R} and \mathcal{R}_H , respectively, hence distinguished by the so-called cut-constructible terms. We remark that within the FDF this distinction is pointless and has been performed only to improve the readability of the formulas. Indeed within the FDF the two contributions are computed simultaneously from the same cuts.

The coefficients c 's entering in the decompositions (32) and (34) can be obtained by using the generalized unitarity techniques for quadruple [4, 56], triple [56–58], and double [59–61] cuts. We observe that single-cut techniques [62–64] are not needed because of the absence of (d -dimensional) massive particles in the loop. In general, the cut $C_{i_1 \dots i_k}$, defined by the conditions $D_{i_1} = \dots = D_{i_k} = 0$, allows for the determination of the coefficients $c_{i_1 \dots i_k; n}$.

V. THE gggg AMPLITUDE

As a first example we consider the four-gluon color-ordered helicity amplitude $A_4(1_g^+, 2_g^+, 3_g^+, 4_g^+)$. The latter vanishes at tree-level, while the one-loop contribution is finite, rational and can be obtained from the quadruple cut $C_{1|2|3|4}$ [24, 35, 65–67]. Therefore the relevant tree-level three-point amplitudes are the ones involving either three gluons or two scalars and one gluon. The tree-level amplitudes with two gluons and one scalar should be included as well but they are not needed since their cut diagrams vanish because of the (-2ϵ) -SRs, see the discussion below. The tree-level are computed by using the color-ordered Feynman rules collected in Appendix C.

The general expression of the three-point all-gluon amplitude is given by

$$\begin{array}{c} \text{1}^{\lambda_1} \\ \text{2}^{\lambda_2} \text{---} \text{3}^{\lambda_3} \end{array} = \frac{ig}{\sqrt{2}} \left[g^{\mu\nu} (\mathbf{1} - 2)^\sigma + g^{\nu\sigma} (2 - \mathbf{3})^\mu + g^{\sigma\mu} (\mathbf{3} - \mathbf{1})^\nu \right] \varepsilon_\mu^{\lambda_1}(\mathbf{1}) \varepsilon_\nu^{\lambda_2}(2, r_2) \varepsilon_\sigma^{\lambda_3}(\mathbf{3}). \quad (35)$$

Generalized massive momenta, carrying dependence on μ , are denoted by a bold font, and the polarization of the particle will be the superscript of the corresponding momentum. The momenta are outgoing,

$$\mathbf{1} + \mathbf{2} + \mathbf{3} = 0, \quad (36)$$

and in general \hat{q}_1 and \hat{q}_3 can be chosen to be proportional,

$$\hat{q}_3 = \xi \hat{q}_1. \quad (37)$$

Moreover the spinors associated to the momenta \mathbf{j}^b and \hat{q}_j are such that

$$\langle \mathbf{j}^b | \hat{q}_j \rangle = [\hat{q}_j | \mathbf{j}^b] = \mu, \quad \mathbf{j} = \mathbf{1}, \mathbf{3}. \quad (38)$$

The polarization vector associated to a massless momentum k is defined as [68]

$$\varepsilon_+^\mu(k, r_k) = \frac{\langle r_k | \gamma^\mu | k \rangle}{\sqrt{2} \langle r_k k \rangle}, \quad \varepsilon_-^\mu(k, r_k) = -\frac{[r_k | \gamma^\mu | k \rangle}{\sqrt{2} [r_k k]}, \quad (39)$$

in terms of an arbitrary reference spinor r_k . We observe that the amplitude (35) is independent of the choice of r_2 . The proof proceeds along the lines of a similar proof presented in Ref. [69]. A change in the reference momentum shifts the amplitude (35) by an amount proportional to

$$[g^{\mu\nu} (1-2)^\sigma + g^{\nu\sigma} (2-3)^\mu + g^{\sigma\mu} (3-1)^\nu] \varepsilon_\mu^{\lambda_1}(1) 2_\nu \varepsilon_\sigma^{\lambda_3}(3), \quad (40)$$

which vanishes owing to momentum conservation, Eq. (36), and to the transversality condition (28).

The explicit expressions of the polarized amplitudes in the FDF are:

$$\begin{aligned} & \begin{array}{c} 1^+ \\ \text{gluon} \\ 2^+ \end{array} \begin{array}{c} \text{gluon} \\ 3^+ \end{array} = 0, \\ & \begin{array}{c} 1^+ \\ \text{gluon} \\ 2^+ \end{array} \begin{array}{c} \text{gluon} \\ 3^- \end{array} = ig \left(\frac{[1^b | 2] [\hat{q}_1 | 2]}{\mu} + \frac{\langle r_2 | 1 | 2 \rangle}{\langle r_2 | 2 \rangle} \right), \\ & \begin{array}{c} 1^0 \\ \text{gluon} \\ 2^+ \end{array} \begin{array}{c} \text{gluon} \\ 3^+ \end{array} = 0, \\ & \begin{array}{c} 1^0 \\ \text{gluon} \\ 2^+ \end{array} \begin{array}{c} \text{gluon} \\ 3^- \end{array} = \frac{\sqrt{2} ig [\hat{q}_1 | 2]^2}{\mu}, \\ & \begin{array}{c} 1^- \\ \text{gluon} \\ 2^+ \end{array} \begin{array}{c} \text{gluon} \\ 3^- \end{array} = ig \frac{[\hat{q}_1 | 2] [\hat{q}_3 | 2] \langle 1^b | 3^b \rangle}{\mu^2}, \\ & \begin{array}{c} 1^0 \\ \text{gluon} \\ 2^+ \end{array} \begin{array}{c} \text{gluon} \\ 3^0 \end{array} = -ig \frac{\langle r_2 | 1 | 2 \rangle}{\langle r_2 | 2 \rangle} \left\{ 1 - \frac{(1+\xi)}{\xi \mu^2} \left[(1+\xi) \mu^2 + \xi \langle \hat{q}_1 | 2 | \hat{q}_1 \rangle \right] \right\}. \end{aligned} \quad (41)$$

The three-point amplitude involving a gluon and two scalars is

$$\begin{aligned} & \begin{array}{c} 1 \\ \text{gluon} \\ 2^+ \end{array} \begin{array}{c} \text{scalar} \\ 3 \end{array} = \frac{ig}{\sqrt{2}} (3-1)^\mu \varepsilon_\mu^{\lambda_2}(2, r_2) G^{AB} \\ & = -ig \frac{\langle r_2 | 1 | 2 \rangle}{\langle r_2 | 2 \rangle} G^{AB}. \end{aligned} \quad (42)$$

The tree-level amplitudes computed above can be used in the cut construction of the one-loop amplitude.

In the FDF, the quadruple-cut $C_{1|2|3|4}$ and the coefficients $c_{1|2|3|4; n}$ can be decomposed into a sum of five contributions,

$$C_{1|2|3|4} = \sum_{i=0}^4 C_{1|2|3|4}^{[i]}, \quad c_{1|2|3|4; n} = \sum_{i=0}^4 c_{1|2|3|4; n}^{[i]}, \quad (43)$$

where $C^{[i]}$ ($c^{[i]}$) is the contribution to the cut (coefficient) involving i internal scalars. In the picture below, internal lines are understood to be on-shell. The quadruple cuts read as follows

$$C_{1|2|3|4}^{[0]} = \begin{array}{c} \text{Diagram 1} \\ \text{Diagram 2} \\ \text{Diagram 3} \end{array}, \quad (44a)$$

$$C_{1|2|3|4}^{[1]} = \sum_{h_i = \pm, 0} \mathcal{T}_1 \begin{array}{c} \text{Diagram 4} \end{array} + \text{c.p.}, \quad (44b)$$

$$C_{1|2|3|4}^{[2]} = \sum_{h_i = \pm, 0} \mathcal{T}_1^2 \begin{array}{c} \text{Diagram 5} \end{array} + \mathcal{T}_2 \begin{array}{c} \text{Diagram 6} \end{array} + \text{c.p.}, \quad (44c)$$

$$C_{1|2|3|4}^{[3]} = \sum_{h_i = \pm, 0} \mathcal{T}_3 \begin{array}{c} \text{Diagram 7} \end{array} + \text{c.p.}, \quad (44d)$$

$$C_{1|2|3|4}^{[4]} = \mathcal{T}_4 \begin{array}{c} \text{Diagram 8} \end{array}, \quad (44e)$$

where the abbreviation “c.p.” means “cyclic permutations of the external particles”. In Eqs. (44), the (-2ϵ) -SR have been stripped off and collected in the prefactors \mathcal{T}_i ,

$$\begin{aligned} \mathcal{T}_1 &= Q^A \hat{G}^{AB} Q^B = 0, \\ \mathcal{T}_2 &= Q^A \hat{G}^{AB} G^{BC} \hat{G}^{CD} Q^D = 0, \\ \mathcal{T}_3 &= Q^A \hat{G}^{AB} G^{BC} \hat{G}^{CD} G^{DE} \hat{G}^{EF} Q^F = 0, \\ \mathcal{T}_4 &= \text{tr} \left(G \hat{G} G \hat{G} G \hat{G} G \hat{G} \right) = -1. \end{aligned} \quad (45)$$

The prefactors $\mathcal{T}_1, \dots, \mathcal{T}_3$ force the cuts (44b) - (44d) to vanish identically. The only cuts contributing, Eqs. (44a) and (44e), lead to the following coefficients

$$\begin{aligned} c_{1|2|3|4;0}^{[0]} &= 0, & c_{1|2|3|4;4}^{[0]} &= 3i \frac{[12][34]}{\langle 12 \rangle \langle 34 \rangle}, \\ c_{1|2|3|4;0}^{[4]} &= 0, & c_{1|2|3|4;4}^{[4]} &= -i \frac{[12][34]}{\langle 12 \rangle \langle 34 \rangle}. \end{aligned} \quad (46)$$

Therefore the only non-vanishing coefficient, $c_{1|2|3|4;4}$, is

$$c_{1|2|3|4;4} = c_{1|2|3|4;4}^{[0]} + c_{1|2|3|4;4}^{[4]} = 2i \frac{[12][34]}{\langle 12 \rangle \langle 34 \rangle}. \quad (47)$$

The color-ordered one-loop amplitude can be obtained from Eq. (32), which in this simple case reduces to

$$\begin{aligned} A_4(1_g^+, 2_g^+, 3_g^+, 4_g^+) &= c_{1|2|3|4;4} I_{1|2|3|4}[\mu^4] \\ &= -\frac{i}{48\pi^2} \frac{[12][34]}{\langle 12 \rangle \langle 34 \rangle}, \end{aligned} \quad (48)$$

and is in agreement with the literature [65]. This example clearly shows the difference between our computation and the one based on the supersymmetric decomposition [67]. In the latter one, the result is uniquely originated by the complex scalar contribution. Instead in our procedure the result arises from both the massive gluons and the massive scalars s_g .

VI. THE $ggq\bar{q}$ AMPLITUDE

In this section we apply generalized-unitarity methods within the FDF scheme to a more involved $2 \rightarrow 2$ process. In particular we show the calculation of the leading color one-loop contribution to the helicity amplitude $A_4(1_g^-, 2_g^+, 3_{\bar{q}}^-, 4_q^+)$, which at tree-level reads,

$$A_4^{\text{tree}} = -i \frac{\langle 13 \rangle^3 \langle 14 \rangle}{\langle 12 \rangle \langle 23 \rangle \langle 34 \rangle \langle 41 \rangle}. \quad (49)$$

The leading-color contribution to a one-loop amplitude with n particles and two external fermions can be decomposed in terms of primitive amplitudes [70]. Following the notation of Ref. [34], we have

$$A_4^{\text{1 loop}} = A_4^L - \frac{1}{N_c^2} A_4^R + \frac{N_f}{N_c} A_4^{L,[1/2]} + \frac{N_s}{N_c} A_4^{L,[0]}, \quad (50)$$

where N_c is the number of colors while N_f (N_s) the number of fermions (scalars). For the helicity configuration we consider both $A_4^{L,[1/2]}$ and $A_4^{L,[0]}$ vanish, thus we will only focus on the contributions of the left-turning amplitude A_4^L and on the right-turning one, A_4^R . The Feynman diagrams leading to the relevant tree-level amplitudes are shown in Appendix E. They are computed by using the color-ordered Feynman rules collected in Appendix C.

Left-turning amplitude – The quadruple cut is given by

$$\begin{aligned} C_{1|2|3|4}^{[L]} &= \text{diagram 1} + \text{diagram 2} + \text{diagram 3} + \text{diagram 4}, \\ c_{1|2|3|4;0}^{[L]} &= \frac{1}{2} A_4^{\text{tree}} \left(1 - \frac{s_{14}^3}{s_{13}^3} \right) s_{12} s_{14}, \\ c_{1|2|3|4;4}^{[L]} &= 0. \end{aligned} \quad (51)$$

The first two cut diagrams contribute to both the cut-constructible and to the rational part, while the last two cut diagrams cancel against each other.

The triple cuts are given by

$$\begin{aligned} C_{12|3|4}^{[L]} &= \text{diagram 1} + \text{diagram 2} + \text{diagram 3} + \text{diagram 4} + \text{diagram 5} + \text{diagram 6}, \\ c_{12|3|4;0}^{[L]} &= \frac{1}{2} A_4^{\text{tree}} \left(1 - \frac{s_{14}^3}{s_{13}^3} \right) s_{12}, \\ c_{12|3|4;2}^{[L]} &= \frac{1}{2} A_4^{\text{tree}} \left(2 - \frac{s_{12}^2}{s_{13}^2} \right); \end{aligned} \quad (52a)$$

$$\begin{aligned} C_{1|2|34}^{[L]} &= \text{diagram 1} + \text{diagram 2} + \text{diagram 3} + \text{diagram 4}, \\ c_{1|2|34;0}^{[L]} &= -\frac{1}{2} A_4^{\text{tree}} \left(1 + \frac{s_{14}^3}{s_{13}^3} \right) s_{12}, \\ c_{1|2|34;2}^{[L]} &= -\frac{1}{2} A_4^{\text{tree}} \frac{s_{12}^2}{s_{13}^2}; \end{aligned} \quad (52b)$$

$$\begin{aligned} C_{1|23|4}^{[L]} &= \text{diagram 1} + \text{diagram 2} + \text{diagram 3}, \\ c_{1|23|4;0}^{[L]} &= -\frac{1}{2} A_4^{\text{tree}} \left(1 + \frac{s_{14}^3}{s_{13}^3} \right) s_{14}, \\ c_{1|23|4;2}^{[L]} &= -\frac{1}{2} A_4^{\text{tree}} \frac{s_{14} s_{12}}{s_{13}^2}; \end{aligned} \quad (52c)$$

$$\begin{aligned}
C_{2|3|41}^{[L]} &= \text{diagram 1} + \text{diagram 2} + \text{diagram 3}, \\
c_{2|3|41;0}^{[L]} &= -\frac{1}{2}A_4^{\text{tree}} \left(1 + \frac{s_{14}^3}{s_{13}^3}\right) s_{14}, \\
c_{2|3|41;2}^{[L]} &= -\frac{1}{2}A_4^{\text{tree}} \frac{s_{14}s_{12}}{s_{13}^2}.
\end{aligned} \tag{52d}$$

In all the triple cuts the last two cut diagrams cancel against each other. In the cut $C_{12|3|4}^{[L]}$, Eq. (52c), the third cut diagram exactly compensates the contribution of the fourth one.

The double cuts read as follows

$$\begin{aligned}
C_{12|34}^{[L]} &= \text{diagram 1} + \text{diagram 2} + \text{diagram 3} \\
&\quad + \text{diagram 4} + \text{diagram 5}, \\
c_{12|34;0}^{[L]} &= A_4^{\text{tree}} \frac{s_{14}}{s_{13}} \left(\frac{s_{14}}{s_{13}} - \frac{1}{2} \right), \\
c_{12|34;2}^{[L]} &= 0;
\end{aligned} \tag{53a}$$

$$\begin{aligned}
C_{23|41}^{[L]} &= \text{diagram 1} + \text{diagram 2} \\
&\quad + \text{diagram 3} + \text{diagram 4}, \\
c_{23|41;0}^{[L]} &= A_4^{\text{tree}} \left(\frac{3}{2} - \frac{s_{14}^2}{s_{13}^2} + \frac{1}{2} \frac{s_{14}}{s_{13}} \right), \\
c_{23|41;2}^{[L]} &= 0.
\end{aligned} \tag{53b}$$

In both cases the last two diagrams cancel against each other. In the case of the cut $C_{13}^{[L]}$ the second and the third diagram cancel as well.

Right-turning amplitude – The quadruple cut is given by

$$\begin{aligned}
C_{1|2|3|4}^{[R]} &= \text{diagram 1} + \text{diagram 2} + \text{diagram 3}, \\
c_{1|2|3|4;0}^{[R]} &= -\frac{1}{2}A_4^{\text{tree}} \frac{s_{12}^3}{s_{13}^3} s_{12} s_{14}, \\
c_{1|2|3|4;4}^{[R]} &= 0.
\end{aligned} \tag{54}$$

The first helicity configuration contributes only to the cut-constructible part while the second one cancels against the box with internal scalars.

The triple cuts are given by

$$\begin{aligned}
C_{12|3|4}^{[R]} &= \text{diagram 1} + \text{diagram 2} \\
&\quad + \text{diagram 3} + \text{diagram 4}, \\
c_{12|3|4;0}^{[R]} &= -\frac{1}{2}A_4^{\text{tree}} \left(2 + \frac{s_{12}^3}{s_{13}^3}\right) s_{12}, \\
c_{12|3|4;2}^{[R]} &= -\frac{1}{2}A_4^{\text{tree}} \left(1 + \frac{s_{14}^2}{s_{13}^2}\right);
\end{aligned} \tag{55a}$$

$$\begin{aligned}
C_{1|2|34}^{[R]} &= \text{diagram 1} + \text{diagram 2}, \\
c_{1|2|34;0}^{[R]} &= -\frac{1}{2}A_4^{\text{tree}} \frac{s_{12}^3}{s_{13}^3} s_{12}, \\
c_{1|2|34;2}^{[R]} &= -\frac{1}{2}A_4^{\text{tree}} \frac{s_{12}}{s_{13}} \left(1 - \frac{s_{14}}{s_{13}}\right);
\end{aligned} \tag{55b}$$

$$\begin{aligned}
C_{1|23|4}^{[R]} &= \text{diagram 1} + \text{diagram 2} + \text{diagram 3}, \\
c_{1|23|4;0}^{[R]} &= -\frac{1}{2}A_4^{\text{tree}} \frac{s_{12}^3}{s_{13}^3} s_{14}, \\
c_{1|23|4;2}^{[R]} &= -\frac{1}{2}A_4^{\text{tree}} \frac{s_{12}s_{14}}{s_{13}^2};
\end{aligned} \tag{55c}$$

$$\begin{aligned}
C_{2|3|41}^{[R]} &= \text{diagram 1} + \text{diagram 2} + \text{diagram 3}, \\
c_{2|3|41;0}^{[R]} &= -\frac{1}{2}A_4^{\text{tree}} \frac{s_{12}^3}{s_{13}^3} s_{14}, \\
c_{2|3|41;2}^{[R]} &= -\frac{1}{2}A_4^{\text{tree}} \frac{s_{12}s_{14}}{s_{13}^2}.
\end{aligned} \tag{55d}$$

In the case of the cuts $C_{12|3|4}^{[R]}$ and $C_{1|2|34}^{[R]}$ the first diagram gives contributions to the both cut-constructible and the rational part, while the second one contributes to the rational part only. In the cuts $C_{12|3|4}^{[R]}$, $C_{1|23|4}^{[R]}$ and $C_{2|3|41}^{[R]}$ the last two diagrams cancel against each other, i.e. the scalar contribution exactly compensates the contribution of the longitudinal polarization of the gluon. The double cuts are

$$\begin{aligned}
C_{12|34}^{[R]} &= \text{diagram 1}, \\
c_{12|34;0}^{[R]} &= A_4^{\text{tree}} \left[\frac{s_{12}}{s_{13}} \left(\frac{s_{14}}{s_{13}} + \frac{3}{2} \right) + \frac{3}{2} \right], \\
c_{12|34;2}^{[R]} &= 0;
\end{aligned} \tag{56a}$$

$$C_{23|41}^{[R]} = \begin{array}{c} \text{Diagram 1} \\ + \\ \text{Diagram 2} \\ + \\ \text{Diagram 3} \end{array},$$

$$c_{23|41;0}^{[R]} = -A_4^{\text{tree}} \frac{s_{12}}{s_{13}} \left(\frac{s_{14}}{s_{13}} + \frac{3}{2} \right),$$

$$c_{23|41;2}^{[R]} = 0. \quad (56b)$$

For the cut $C_{24}^{[R]}$, the first diagram contributes to the cut-constructible part only while the second one is cancelled by the diagram with an internal scalar.

Leading-color amplitude – The leading color amplitude can be obtained from the decomposition (32) by using the coefficients

$$c_{i_1 \dots i_k; n} = c_{i_1 \dots i_k; n}^{[L]} - \frac{1}{N_c^2} c_{i_1 \dots i_k; n}^{[R]}, \quad (57)$$

and the explicit expression of the MIs, Eq. (D1). The result agrees with the one presented in Ref. [65].

VII. THE ggH AMPLITUDE

In this section, we show the calculation of the leading color one-loop contribution to the helicity amplitude $A_4(1_g^-, 2_g^+, 3_g^+, H)$ in the heavy top-mass limit. This example allows us to show how the FDF scheme can be applied in the context of an effective theory, where the Higgs boson couples directly to the gluon. The Feynman rules for the Higgs-gluon and Higgs-scalar couplings in the FDF are given in Appendix C. They are used to compute the tree-level amplitudes sewn along the cuts. The tree-level amplitudes are not shown, but they can be easily obtained by using a construction similar to the one used in Appendix E. In the following we present directly the determination of the coefficients by means of generalized unitarity methods.

The leading-order contribution reads as follows

$$A_{4,H}^{\text{tree}} = i \frac{[23]^4}{[12][23][31]}. \quad (58)$$

The quadruple cuts are given by:

$$C_{1|2|3|H} = \begin{array}{c} \text{Diagram 1} \\ + \\ \text{Diagram 2} \end{array},$$

$$c_{1|2|3|H;0} = -\frac{1}{2} A_{4,H}^{\text{tree}} s_{12} s_{23},$$

$$c_{1|2|3|H;4} = 0; \quad (59a)$$

$$C_{1|2|H|3} = \begin{array}{c} \text{Diagram 1} \\ + \\ \text{Diagram 2} \end{array},$$

$$c_{1|2|H|3;0} = -\frac{1}{2} A_{4,H}^{\text{tree}} s_{13} s_{12},$$

$$c_{1|2|H|3;4} = 0; \quad (59b)$$

$$C_{1|H|2|3} = \begin{array}{c} \text{Diagram 1} \\ + \\ \text{Diagram 2} \end{array},$$

$$c_{1|H|2|3;0} = -\frac{1}{2} A_{4,H}^{\text{tree}} s_{23} s_{13},$$

$$c_{1|H|2|3;4} = 0. \quad (59c)$$

The triple cuts with two massive channels are

$$C_{12|3|H} = \begin{array}{c} \text{Diagram 1} \\ + \\ \text{Diagram 2} \end{array},$$

$$c_{12|3|H;0} = \frac{1}{2} A_{4,H}^{\text{tree}} (s_{13} + s_{23}),$$

$$c_{12|3|H;2} = 0; \quad (60a)$$

$$C_{12|H|3} = \begin{array}{c} \text{Diagram 1} \\ + \\ \text{Diagram 2} \end{array},$$

$$c_{12|H|3;0} = \frac{1}{2} A_{4,H}^{\text{tree}} (s_{13} + s_{23}),$$

$$c_{12|H|3;2} = 0; \quad (60b)$$

$$C_{1|23|H} = \begin{array}{c} \text{Diagram 1} \\ + \\ \text{Diagram 2} \end{array},$$

$$c_{1|23|H;0} = \frac{1}{2} A_{4,H}^{\text{tree}} (s_{12} + s_{13}),$$

$$c_{1|23|H;2} = 0; \quad (60c)$$

$$C_{1|H|23} = \begin{array}{c} \text{Diagram 1} \\ + \\ \text{Diagram 2} \end{array},$$

$$c_{1|H|23;0} = \frac{1}{2} A_{4,H}^{\text{tree}} (s_{12} + s_{13}),$$

$$c_{1|H|23;2} = 0; \quad (60d)$$

$$C_{2|H|31} = \begin{array}{c} \text{Diagram 1} \\ + \\ \text{Diagram 2} \end{array},$$

$$c_{2|H|31;0} = \frac{1}{2} A_{4,H}^{\text{tree}} (s_{12} + s_{23}),$$

$$c_{2|H|31;2} = 0; \quad (60e)$$

$$C_{H|2|31} = \begin{array}{c} \text{Diagram 1} \\ + \\ \text{Diagram 2} \end{array},$$

$$c_{H|2|31;0} = \frac{1}{2} A_{4,H}^{\text{tree}} (s_{12} + s_{23}),$$

$$c_{H|2|31;2} = 0; \quad (60f)$$

while the ones with one massive channel only read as follows:

$$C_{1|2|3H} = \text{diagram} + \text{diagram},$$

$$c_{1|2|3H;0} = 0,$$

$$c_{1|2|3H;2} = 0; \quad (61a)$$

$$C_{1|2H|3} = \text{diagram} + \text{diagram},$$

$$c_{1|2H|3;0} = 0,$$

$$c_{1|2H|3;2} = 0; \quad (61b)$$

$$C_{1H|2|3} = \text{diagram} + \text{diagram},$$

$$c_{1H|2|3;0} = 0,$$

$$c_{1H|2|3;2} = -2A_{4,H}^{\text{tree}} \frac{s_{12}s_{13}}{s_{23}^2}. \quad (61c)$$

Finally the double cuts are given by:

$$C_{12|3H} = \text{diagram} + \text{diagram},$$

$$c_{12|3H;0} = 0,$$

$$c_{12|3H;2} = 0; \quad (62a)$$

$$C_{23|H1} = \text{diagram} + \text{diagram},$$

$$c_{23|H1;0} = 0,$$

$$c_{23|H1;2} = 4A_{4,H}^{\text{tree}} \frac{s_{12}s_{13}}{s_{23}^3}; \quad (62b)$$

$$C_{H2|31} = \text{diagram} + \text{diagram},$$

$$c_{H2|31;0} = 0,$$

$$c_{H2|31;2} = 0. \quad (62c)$$

The cut $C_{123|H}$ does not give any contribution.

Finally, the one-loop amplitude can be obtained by using the coefficients collected in Eqs. (59) - (62) and the decomposition (34). The result agrees with the literature [71].

VIII. GENERALIZED OPEN LOOP

The FDF of d -dimensional one-loop amplitudes is compatible with methods generating recursively the integrands of one-loop amplitudes [72, 73] and leads to the *complete reconstruction* of the numerator of Feynman integrands as a polynomial in the loop variables, ℓ^ν and μ . Our scheme allows for a generalization of the current implementations of these techniques [38–40]. Indeed, currently the latter can reconstruct only the four-dimensional part the numerator of the integrands, which is polynomial in ℓ^ν only. In the following we focus on the generalization of the *open-loop* technique [38] within the FDF scheme.

Tree-level and one-loop amplitudes, \mathcal{M} and $\delta\mathcal{M}$, can be obtained as a sum of Feynman diagrams

$$\mathcal{M} = \sum_{\text{diag}} \mathcal{M}^{(\text{diag})} \quad \delta\mathcal{M} = \sum_{\text{diag}} \delta\mathcal{M}^{(\text{diag})}. \quad (63)$$

The color factor \mathcal{C} and the (-2ϵ) -SRs term \mathcal{T} factorize, thus they can be stripped off each diagram

$$\mathcal{M}^{(\text{diag})} = \mathcal{C}^{(\text{diag})} \mathcal{A}^{(\text{diag})}$$

$$\delta\mathcal{M}^{(\text{diag})} = \mathcal{C}^{(\text{diag})} \mathcal{T}^{(\text{diag})} \mathcal{A}^{(\text{diag})}. \quad (64)$$

The color structures are computed once, as described in [38]. The computation of the (-2ϵ) -SRs prefactors \mathcal{T} turns out to be even easier, since they enter only in the one-loop diagrams and can be computed once and for all. In the 't Hooft-Feynman gauge they can be either 0 or 1.

The recursive construction of the color-stripped tree-level diagrams, $\mathcal{A}^{(\text{diag})}$, is not affected by the new Feynman particles and Feynman rules, which enter at loop-level only.

The one-loop color-stripped diagram $\delta\mathcal{A}^{(\text{diag})}$, characterized by a given topology \mathcal{I}_n , is constructed by n tree-level topologies i_1, \dots, i_n , connected to the loop. The numerator of the one-loop diagram can be expressed as

$$\mathcal{N}(\mathcal{I}_n, \ell, \mu) = \sum_{j=0}^R \sum_{a=0}^{R-j} \mathcal{N}_{\nu_1 \dots \nu_j}^{[a]}(\mathcal{I}_n) \ell^{\nu_1} \dots \ell^{\nu_j} \mu^a, \quad (65)$$

where R is its rank. The diagram is obtained by performing the integration over the d -dimensional loop momentum:

$$\delta\mathcal{A}^{(\text{diag})} = \sum_{j=0}^R \sum_{a=0}^{R-j} \mathcal{N}_{\nu_1 \dots \nu_j}^{[a]}(\mathcal{I}_n) I_n^{\nu_1 \dots \nu_j} [\mu^a], \quad (66)$$

where

$$I_n^{\nu_1 \dots \nu_j} [\mu^a] \equiv \int d^d \bar{\ell} \frac{\ell^{\nu_1} \dots \ell^{\nu_j} \mu^a}{D_0 \dots D_{n-1}}. \quad (67)$$

The starting point of the open-loop technique is to cut a propagator and to remove the denominators. The open

numerator can be expressed in terms of the tree-level topology i_n and a one loop topology \mathcal{I}_{n-1} :

$$\mathcal{N}_{\alpha}^{\beta}(\mathcal{I}_n, \ell, \mu) = X_{\gamma\delta}^{\beta}(\mathcal{I}_n, i_n, \mathcal{I}_{n-1}) \mathcal{N}_{\alpha}^{\gamma}(\mathcal{I}_{n-1}, \ell, \mu) \omega^{\delta}(i_n), \quad (68)$$

where ω^{δ} is the expression related to the tree-level topology i_n . The vertices $X_{\gamma\delta}^{\beta}$ are obtained by the FDF Feynman rules, Eqs. (13), and can be written as follows,

$$X_{\gamma\delta}^{\beta} = Y_{\gamma\delta}^{\beta} + \ell^{\nu} Z_{\nu; \gamma\delta}^{\beta} + \mu W_{\gamma\delta}^{\beta}. \quad (69)$$

Therefore the tensor coefficients of the covariant decomposition

$$\mathcal{N}_{\alpha}^{\beta}(\mathcal{I}_n, \ell, \mu) = \sum_{j=0}^R \sum_{a=0}^{R-j} \mathcal{N}_{\nu_1 \dots \nu_j; \alpha}^{[a]\beta}(\mathcal{I}_n) \ell^{\nu_1} \dots \ell^{\nu_j} \mu^a$$

are obtained by the recursive relation

$$\begin{aligned} \mathcal{N}_{\nu_1 \dots \nu_j; \alpha}^{[a]\beta}(\mathcal{I}_n) &= [Y_{\gamma\delta}^{\beta} \mathcal{N}_{\nu_1 \dots \nu_j; \alpha}^{[a]\beta}(\mathcal{I}_{n-1}) \\ &+ Z_{\nu_1; \gamma\delta}^{\beta} \mathcal{N}_{\nu_2 \dots \nu_j; \alpha}^{[a]\beta}(\mathcal{I}_{n-1}) \\ &+ W_{\gamma\delta}^{\beta} \mathcal{N}_{\nu_1 \dots \nu_j; \alpha}^{[a-1]\beta}(\mathcal{I}_{n-1})] \omega^{\delta}(i_n). \end{aligned} \quad (70)$$

The recursive generation of integrands within the FDF can be suitably combined with public codes like SAMURAI [74] and NINJA [75, 76], which can reduce integrands keeping the full dependence on the loop variables ℓ^{ν} and μ . Moreover it can improve the generation of the d -dimensional integrands performed by the packages GoSAM [77] and FORMCALC [45]. The latter are public codes dedicated to the automatic evaluation of one-loop multi-particle scattering amplitudes, and they already support the FDH regularization scheme.

IX. CONCLUSIONS

We introduced a four-dimensional formulation (FDF) of the d -dimensional regularization of one-loop scattering amplitudes. Within our FDF, particles that propagate inside the loop are represented by massive particles regularizing the divergences. Their interactions are described by generalized four-dimensional Feynman rules. They include selection rules accounting for the regularization of the amplitudes. In particular, massless spin-1 particles in d -dimensions were represented in four-dimensions by a combination of massive spin-one particle and a scalar particle. Fermions in d -dimensions were represented by four-dimensional fermions obeying the Dirac equation for tachyonic particles. The integrands of one-loop amplitudes in the FDF and in the FDH scheme differ by spurious terms which vanish upon integration over the loop momentum. Therefore the two schemes are equivalent.

In the FDF, the polarization and helicity states of the particles inside the loop admit an explicit four-dimensional representation, allowing for a complete,

four-dimensional, unitarity-based construction of d -dimensional amplitudes. The application of generalized-unitarity methods within the FDF has been described in detail by computing the NLO QCD corrections to helicity amplitudes of the processes $gg \rightarrow q\bar{q}$, and $gg \rightarrow gH$. Mutual cancellations among the contributions of the longitudinal gluons and the ones of the scalar particles suggest a connection among them that deserves further investigations.

The FDF Feynman rules are compatible with methods generating recursively the integrands of one-loop amplitudes. In this context we have proposed a generalization to the open loop method, which allows for a complete reconstruction of the integrand, currently limited to four dimensions only.

The FDF approach is suitable for analytic as well as numerical implementation. Its main asset is the use of purely four-dimensional ingredients for the complete reconstruction of dimensionally-regulated one-loop amplitudes. We plan to investigate its applicability beyond one loop. In particular we aim at using explicit four-dimensional representations to avoid the complications emerging from the formal manipulations of the $(d-4)$ -dimensional degrees of freedom.

Acknowledgments

We wish to thank Francesco Buciuni for cross-checking parts of the results. A.R.F. and W.J.T. thank the Max-Planck-Institute for Physics in Munich for the kind hospitality at several stages of this project. For the same reasons, E.M. wishes to thank the Department of Mathematics and Physics of the University of Salento.

A.R.F. is partially supported by the UNAL-DIB grant N. 20629 of the “Convocatoria del programa nacional de proyectos para el fortalecimiento de la investigación, la creación y la innovación en posgrados de la Universidad Nacional de Colombia 2013-2015”.

The work of P.M. is supported by the Alexander von Humboldt Foundation, in the framework of the Sofja Kovaleskaja Award Project “Advanced Mathematical Methods for Particle Physics”, endowed by the German Federal Ministry of Education and Research.

W.J.T. is supported by Fondazione Cassa di Risparmio di Padova e Rovigo (CARIPARO).

Appendix A: One-loop equivalence

In this Appendix we show that, at one loop, the FDH scheme defined by Eqs. (2) – (5b) is equivalent to the one defined by Eqs. (2) – (5a) and (10).

In the two approaches the only differences may arise from the manipulations of the -2ϵ components of the Dirac matrices contracted among each others. Therefore potential differences in their predictions can only be rational contributions of divergent diagrams involving at

least an open fermion line. The loop-dependent part of the integrand of a one-loop diagram is a sum of integrands of the type

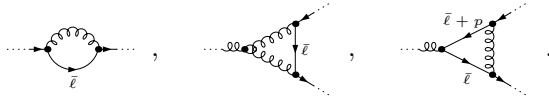
$$\mathcal{I}_{r,a,k} \equiv \frac{\ell^{\mu_1} \dots \ell^{\mu_r} (\mu^2)^a}{D_{i_1} \dots D_{i_k}},$$

$$D_j \equiv (\ell + p_j)^2 - m_j^2 - \mu^2. \quad (\text{A1})$$

An integrand $\mathcal{I}_{r,a,k}$ leads to a divergent integral if it satisfies the conditions

$$4 + r + 2a - 2k \geq 0. \quad (\text{A2})$$

At one loop in QCD the diagrams involving at least an open fermion line and integrands fulfilling the conditions (A2) are



For these diagrams, the numerators obtained by using the two schemes differ by terms of the type

$$\dots \tilde{\gamma}^\alpha (\ell + \tilde{\ell} + m) \tilde{\gamma}_\alpha \dots,$$

$$\dots \tilde{\gamma}^\alpha (\ell + \tilde{\ell} + m) \gamma^\mu (\ell + p + \tilde{\ell} + m) \tilde{\gamma}_\alpha \dots, \quad (\text{A3})$$

where “...” represent four dimensional spinorial objects. In the FDH scheme it is easy to show that the terms (A3) vanish in the $d_s \rightarrow 4$ limit, while in the other scheme they vanish as a consequence of Eq. (10). Therefore the two sets of prescriptions lead to the same integrand.

The FDF fulfills the prescriptions (2) – (5a) and (10), thus, at one loop, it leads to the same amplitudes of the FDH scheme.

Appendix B: Proof of the completeness relations

In this Appendix we show that the generalized spinors (20) fulfill the completeness relation (19). For later convenience we define the chirality projectors

$$\omega_\pm = \frac{\mathbb{I} \pm \gamma^5}{2}, \quad (\text{B1})$$

and we show that:

$$\frac{|q_\ell|[\ell^b] - |l^b][q_\ell]}{[\ell^b q_\ell]} =$$

$$= \frac{|q_\ell| \langle q_\ell \ell^b \rangle [\ell^b] + |\ell^b| \langle \ell^b q_\ell \rangle [q_\ell]}{2\ell^b \cdot q_\ell}$$

$$= \frac{(|q_\ell| \langle q_\ell \rangle)(|\ell^b| [\ell^b]) + (|\ell^b| \langle \ell^b \rangle)(|q_\ell| [q_\ell])}{2\ell^b \cdot q_\ell}$$

$$= \frac{\omega_- \not{q}_\ell \omega_+ \not{\ell}^b + \omega_- \not{\ell}^b \omega_+ \not{q}_\ell}{2\ell^b \cdot q_\ell}$$

$$= \frac{\omega_-^2 \{\not{q}_\ell \not{\ell}^b\}}{2\ell^b \cdot q_\ell} = \omega_-, \quad (\text{B2a})$$

and similarly

$$\frac{|\ell^b| \langle q_\ell \rangle - |q_\ell| \langle \ell^b \rangle}{\langle q_\ell \ell^b \rangle} = \omega_+. \quad (\text{B2b})$$

Using Eqs. (B2) we get

$$\sum_{\lambda=\pm} u_\lambda(\ell) \bar{u}_\lambda(\ell) =$$

$$= \left(|\ell^b| + \frac{(m-i\mu)}{[\ell^b q_\ell]} |q_\ell| \right) \left(|\ell^b| + \frac{(m+i\mu)}{\langle q_\ell \ell^b \rangle} \langle q_\ell \rangle \right) +$$

$$\left(|\ell^b| + \frac{(m+i\mu)}{\langle \ell^b q_\ell \rangle} |q_\ell| \right) \left(\langle \ell^b \rangle + \frac{(m-i\mu)}{[q_\ell \ell^b]} [q_\ell] \right)$$

$$= \not{\ell}^b + \frac{m^2 + \mu^2}{2\ell^b \cdot q_\ell} \not{q}_\ell + (m-i\mu) \frac{|q_\ell|[\ell^b] - |\ell^b][q_\ell]}{[\ell^b q_\ell]}$$

$$+ (m+i\mu) \frac{|\ell^b| \langle q_\ell \rangle - |q_\ell| \langle \ell^b \rangle}{\langle q_\ell \ell^b \rangle}$$

$$\stackrel{\text{Eq. (B2)}}{=} \not{\ell}^b + \frac{m^2 + \mu^2}{2\ell^b \cdot q_\ell} \not{q}_\ell + (m-i\mu)\omega_- + (m+i\mu)\omega_+$$

$$\stackrel{\text{Eq. (17)}}{=} \not{\ell} + i\mu\gamma^5 + m. \quad (\text{B3})$$

Appendix C: Color-ordered Feynman rules

In the FDF, the d -dimensional color-ordered Feynman rules collected in Ref. [68] become:

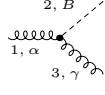
$$\text{gluon} \quad \bullet_\alpha \text{---}^k \text{---} \bullet_\beta = -i \frac{g^{\alpha\beta}}{k^2 - \mu^2 + i0}, \quad (\text{C1a})$$

$$\text{scalar} \quad \bullet_A \text{---}^k \text{---} \bullet_B = -i \frac{G^{AB}}{k^2 - \mu^2 + i0}, \quad (\text{C1b})$$

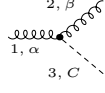
$$\text{fermion} \quad \bullet \text{---}^k \text{---} \bullet = i \frac{\not{k} + i\mu\gamma^5 + m}{k^2 - m^2 - \mu^2 + i0}, \quad (\text{C1c})$$

$$\text{gluon} \quad \begin{matrix} 2, \beta \\ \text{---} \\ 1, \alpha \end{matrix} \text{---}^k \text{---} \begin{matrix} \text{---} \\ 3, \gamma \end{matrix} = \frac{i}{\sqrt{2}} [g_{\alpha\beta}(k_1 - k_2)_\gamma + g_{\beta\gamma}(k_2 - k_3)_\alpha + g_{\gamma\alpha}(k_3 - k_1)_\beta], \quad (\text{C1d})$$

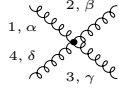
$$\text{gluon} \quad \begin{matrix} 2, B \\ \text{---} \\ 1, \alpha \end{matrix} \text{---}^k \text{---} \begin{matrix} \text{---} \\ 3, C \end{matrix} = \frac{i}{\sqrt{2}} (k_2 - k_3)_\alpha G^{BC}, \quad (\text{C1e})$$



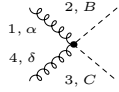
$$= \pm \frac{i}{\sqrt{2}} g_{\alpha\gamma} (i\mu) Q^B, \quad (\tilde{k}_1 = 0, \quad \tilde{k}_3 = \pm \tilde{\ell}) \quad (\text{C1f})$$



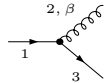
$$= \mp \frac{i}{\sqrt{2}} g_{\alpha\beta} (i\mu) Q^C, \quad (\tilde{k}_1 = 0, \quad \tilde{k}_3 = \pm \tilde{\ell}) \quad (\text{C1g})$$



$$= i g_{\alpha\gamma} g_{\beta\delta} - \frac{i}{2} (g_{\alpha\beta} g_{\gamma\delta} + g_{\alpha\delta} g_{\beta\gamma}), \quad (\text{C1h})$$



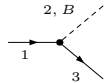
$$= -\frac{i}{2} g_{\alpha\delta} G^{BC}, \quad (\text{C1i})$$



$$= -\frac{i}{\sqrt{2}} \gamma^\beta, \quad (\text{C1j})$$



$$= \frac{i}{\sqrt{2}} \gamma^\beta, \quad (\text{C1k})$$

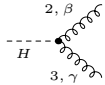


$$= -\frac{i}{\sqrt{2}} \gamma^5 \Gamma^B, \quad (\text{C1l})$$

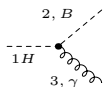


$$= \frac{i}{\sqrt{2}} \gamma^5 \Gamma^B, \quad (\text{C1m})$$

The color-ordered Feynman rules describing the interaction among an external Higgs boson and gluons in the infinite top-mass limit are given by



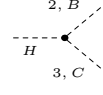
$$= -2i \left[k_3^\beta k_2^\gamma - g^{\beta\gamma} (k_2 \cdot k_3 + \mu^2) \right], \quad (\text{C2a})$$



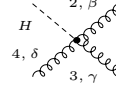
$$= \pm 2 k_2^\gamma \mu Q^B \quad (\tilde{k}_3 = \pm \tilde{\ell}), \quad (\text{C2b})$$



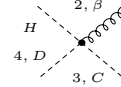
$$= \pm 2 k_3^\beta \mu Q^C \quad (\tilde{k}_2 = \pm \tilde{\ell}), \quad (\text{C2c})$$



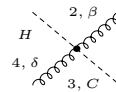
$$= -2i \left[\mu^2 Q^B Q^C - G^{BC} (k_2 \cdot k_3 + \mu^2) \right], \quad (\text{C2d})$$



$$= i\sqrt{2} \left[g_{\beta\gamma} (k_2 - k_3)_\delta + g_{\beta\delta} (k_4 - k_2)_\gamma + g_{\gamma\delta} (k_3 - k_4)_\beta \right], \quad (\text{C2e})$$

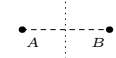


$$= i\sqrt{2} G^{CD} (k_3 - k_4)_\beta, \quad (\text{C2f})$$



$$= \mp \sqrt{2} g_{\beta\delta} \mu Q^C \quad (\tilde{k}_4 - \tilde{k}_2 = \pm \tilde{\ell}). \quad (\text{C2g})$$

In the Feynman rules (C1), (C2) all the momenta are outgoing. The terms μ^2 appearing in the the propagators (C1a)–(C1c) enter only if the corresponding momentum k is d -dimensional, *i.e.* only if k contains the loop momentum $\tilde{\ell}$. In the vertices (C1f), (C1g) the momentum k_1 is four-dimensional while the other two are d -dimensional. For these vertices the overall sign depend on which of the combinations (14) is present in the vertex. Similarly the overall sign of the Feynman rules (C2b), (C2c) and (C2g) depend on the flow of the loop momentum $\tilde{\ell}$. As already mentioned each cut scalar propagator carries a (-2ϵ) -SRs factor of the type



$$= \hat{G}^{AB}, \quad (\text{C3})$$

where \hat{G}^{AB} is defined in Eq. (29).

Appendix D: Master integrals

In this appendix we present the MIs entering in the decomposition of the four-point amplitudes computed in Sections V, VI and VII.

The MIs in the decomposition (32) of the one-loop amplitude of the process (31) are given by

$$I_{1|2|3|4} = \frac{r_\Gamma}{s_{12}s_{14}} \left[\frac{2}{\epsilon^2} ((-s_{12})^{-\epsilon} + (-s_{14})^{-\epsilon}) - \log^2 \left(\frac{-s_{12}}{-s_{14}} \right) - \pi^2 \right],$$

$$I_{ij|k|m} = I_{k|m|ij} = I_{m|ij|k} = -\frac{r_\Gamma}{\epsilon^2 s_{ij}} (-s_{ij})^{-\epsilon},$$

$$\begin{aligned}
I_{ij|km} &= \frac{r_\Gamma}{\epsilon(1-2\epsilon)} (-s_{ij})^{-\epsilon}, \\
I_{1|2|3|4} [\mu^4] &= \frac{4\epsilon(\epsilon-1)I_{1|2|3|4}}{b_0^2(2\epsilon-3)(2\epsilon-1)} \\
&\quad + \frac{b_1(\epsilon-1)}{2\epsilon-3} \left[I_{1|2|34}[\mu^2] - \frac{2\epsilon I_{1|2|34}}{b_0(2\epsilon-1)} \right] \\
&\quad + \frac{b_2(\epsilon-1)}{2\epsilon-3} \left[I_{2|3|41}[\mu^2] - \frac{2\epsilon I_{2|3|41}}{b_0(2\epsilon-1)} \right] \\
&= -\frac{1}{6} + \mathcal{O}(\epsilon), \\
I_{ij|k|m} [\mu^2] &= I_{k|m|ij} [\mu^2] = I_{m|ij|k} [\mu^2] \\
&= -\frac{r_\Gamma (-s_{ij})^{-\epsilon}}{2(1-\epsilon)(1-2\epsilon)} = -\frac{1}{2} + \mathcal{O}(\epsilon), \\
I_{ij|km} [\mu^2] &= \frac{r_\Gamma (-s_{ij})^{1-\epsilon}}{2(1-2\epsilon)(3-2\epsilon)} \\
&= -\frac{1}{6} s_{ij} + \mathcal{O}(\epsilon). \tag{D1}
\end{aligned}$$

The factor r_Γ is defined as

$$r_\Gamma \equiv \frac{\Gamma^2(1-\epsilon)\Gamma(1+\epsilon)}{\Gamma(1-2\epsilon)}, \tag{D2}$$

while the coefficients b read as [24, 78]

$$b_0 = -\frac{4s_{13}}{s_{12}s_{23}}, \quad b_1 = \frac{s_{12}}{s_{13}}, \quad b_2 = \frac{s_{23}}{s_{13}}. \tag{D3}$$

The MIs entering the decomposition (34) for the process (33) are given by

$$\begin{aligned}
I_{i|j|k|H} &= I_{j|i|H|k} = I_{i|H|k|j} \\
&= \frac{2r_\Gamma}{s_{ij}s_{jk}} \frac{1}{\epsilon^2} \left[(-s_{ij})^{-\epsilon} + (-s_{jk})^{-\epsilon} - (m_H^2)^{-\epsilon} \right] \\
&\quad - \frac{2r_\Gamma}{s_{ij}s_{jk}} \left[\text{Li}_2 \left(1 - \frac{m_H^2}{s_{ij}} \right) + \text{Li}_2 \left(1 - \frac{m_H^2}{s_{jk}} \right) \right. \\
&\quad \left. + \frac{1}{2} \log^2 \frac{s_{ij}}{s_{jk}} + \frac{\pi^2}{6} \right], \\
I_{ij|k|H} &= I_{ij|H|k} = I_{k|H|ij} = I_{H|k|ij} = I_{k|ij|H} \\
&= \frac{r_\Gamma (-s_{ij})^{-\epsilon} - (-m_H^2)^{-\epsilon}}{\epsilon^2 (-s_{ij}) - (-m_H^2)}, \\
I_{i|j|kH} &= I_{kH|ij} = I_{i|kH|j} = \frac{r_\Gamma}{\epsilon^2} (-s_{ij})^{-1-\epsilon}, \\
I_{ij|Hk} &= I_{Hk|ij} = I_{ij|kH} = \frac{r_\Gamma}{\epsilon(1-2\epsilon)} (-s_{ij})^{-\epsilon}, \\
I_{123|H} &= \frac{r_\Gamma}{\epsilon(1-2\epsilon)} (-m_H^2)^{-\epsilon}, \\
I_{i|j|k|m} [\mu^4] &= \frac{4\epsilon(\epsilon-1)}{a_0^2(2\epsilon-3)(2\epsilon-1)} I_{i|j|k|m} \\
&\quad + \frac{a_1(\epsilon-1)}{a_0(2\epsilon-3)} \left[I_{j|k|mi} [\mu^2] - \frac{2\epsilon I_{j|k|mi}}{a_0(2\epsilon-1)} \right] \\
&\quad + \frac{a_2(\epsilon-1)}{a_0(2\epsilon-3)} \left[I_{ij|k|m} [\mu^2] - \frac{2\epsilon I_{ij|k|m}}{a_0(2\epsilon-1)} \right]
\end{aligned}$$

$$\begin{aligned}
&\quad + \frac{a_3(\epsilon-1)}{a_0(2\epsilon-3)} \left[I_{i|jk|m} [\mu^2] - \frac{2\epsilon I_{i|jk|m}}{a_0(2\epsilon-1)} \right] \\
&\quad + \frac{a_4(\epsilon-1)}{a_0(2\epsilon-3)} \left[I_{i|j|km} [\mu^2] - \frac{2\epsilon I_{i|j|km}}{a_0(2\epsilon-1)} \right] \\
&= -\frac{1}{6} + \mathcal{O}(\epsilon), \\
I_{ij|k|H} [\mu^2] &= I_{ij|H|k} [\mu^2] = I_{k|H|ij} [\mu^2] \\
&= I_{H|k|ij} [\mu^2] = I_{k|ij|H} [\mu^2] \\
&= \frac{-r_\Gamma}{2(1-\epsilon)(1-2\epsilon)} \frac{(-s_{ij})^{1-\epsilon} - (-m_H^2)^{1-\epsilon}}{(-s_{ij}) - (-m_H^2)} \\
&= -\frac{1}{2} + \mathcal{O}(\epsilon), \\
I_{i|j|kH} [\mu^2] &= I_{kH|ij} [\mu^2] = I_{i|kH|j} [\mu^2] \\
&= \frac{-r_\Gamma (-s_{ij})^{-\epsilon}}{2(1-\epsilon)(1-2\epsilon)} = -\frac{1}{2} + \mathcal{O}(\epsilon), \\
I_{ij|Hk} [\mu^2] &= I_{Hk|ij} [\mu^2] = I_{ij|kH} [\mu^2] \\
&= \frac{r_\Gamma (-s_{ij})^{1-\epsilon}}{2(3-2\epsilon)(1-2\epsilon)} = -\frac{1}{6} s_{ij} + \mathcal{O}(\epsilon), \\
I_{123|H} [\mu^2] &= \frac{r_\Gamma (-m_H^2)^{1-\epsilon}}{2(3-2\epsilon)(1-2\epsilon)} = -\frac{1}{6} m_H^2 + \mathcal{O}(\epsilon), \tag{D4}
\end{aligned}$$

The coefficients a read as follows,

$$a_0 \equiv \sum_{s=1}^4 a_s, \quad a_s \equiv \sum_{t=1}^4 \left(S_{i|j|k|m}^{-1} \right)_{st}, \tag{D5}$$

in terms of the cut-dependent matrix

$$(S_{i|j|k|m})_{st} \equiv -\frac{1}{2} \left(v_{i|j|k|m}^{(s)} - v_{i|j|k|m}^{(t)} \right)^2, \tag{D6}$$

where

$$\begin{aligned}
v_{i|j|k|m}^{(1)} &= 0, & v_{i|j|k|m}^{(2)} &= p_i, \\
v_{i|j|k|m}^{(3)} &= p_i + p_j, & v_{i|j|k|m}^{(4)} &= -p_m. \tag{D7}
\end{aligned}$$

Appendix E: Tree-level amplitudes

In this Appendix we present the three- and four-point tree-level amplitudes entering in the computation described in Section VI. They can be computed by using the Feynman rules collected in Eqs. (C1). The legs with a dot are massive with mass μ .

The tree-level amplitudes entering in the unitarity-based decomposition of the *left-turning amplitudes* amplitude can be expressed in terms of Feynman diagrams as follows:

$$A_3(g \, g^\bullet \, g^\bullet) = \text{diagram}$$

$$A_3(g s_g^\bullet s_g^\bullet) = \text{diagram}$$

$$A_3(g^\bullet \bar{q} q^\bullet) = \text{diagram}$$

$$A_3(g^\bullet \bar{q}^\bullet q) = \text{diagram}$$

$$A_3(s_g^\bullet \bar{q} q^\bullet) = \text{diagram}$$

$$A_3(s_g^\bullet \bar{q}^\bullet q) = \text{diagram}$$

$$A_4(g g g^\bullet g^\bullet) = \text{diagram} + \text{diagram}$$

$$A_4(g^\bullet g^\bullet \bar{q} q) = \text{diagram} + \text{diagram}$$

$$A_4(g^\bullet g \bar{q} q^\bullet) = \text{diagram} + \text{diagram}$$

$$A_4(g g^\bullet \bar{q}^\bullet q) = \text{diagram} + \text{diagram}$$

$$A_4(g g s_g^\bullet s_g^\bullet) = \text{diagram} + \text{diagram}$$

$$A_4(g s_g^\bullet \bar{q}^\bullet q) = \text{diagram} + \text{diagram}$$

$$A_4(s_g^\bullet g \bar{q} q^\bullet) = \text{diagram} + \text{diagram}$$

$$A_4(s_g^\bullet s_g^\bullet \bar{q} q) = \text{diagram} + \text{diagram} \quad (\text{E1})$$

The three- and the four-point tree-level amplitudes entering in the computation of the *right-turning amplitude* are

$$A_3(g \bar{q}^\bullet q^\bullet) = \text{diagram}$$

$$A_3(g^\bullet q^\bullet \bar{q}) = \text{diagram}$$

$$A_3(g^\bullet q \bar{q}^\bullet) = \text{diagram}$$

$$A_3(s_g^\bullet q^\bullet \bar{q}) = \text{diagram}$$

$$A_3(s_g^\bullet q \bar{q}^\bullet) = \text{diagram}$$

$$A_4(g g \bar{q}^\bullet q^\bullet) = \text{diagram} + \text{diagram}$$

$$A_4(\bar{q}^\bullet q^\bullet \bar{q} q) = \text{diagram} + \text{diagram}$$

$$A_4(q^\bullet g \bar{q} g^\bullet) = \text{diagram} + \text{diagram}$$

$$A_4(g \bar{q}^\bullet g^\bullet q) = \text{diagram} + \text{diagram}$$

$$A_4(q^\bullet g \bar{q} s_g^\bullet) = \text{diagram} + \text{diagram}$$

$$A_4(g \bar{q}^\bullet s_g^\bullet q) = \text{diagram} + \text{diagram} \quad (\text{E2})$$

-
- [1] F. Cachazo, P. Svrcek, and E. Witten, JHEP **09**, 006 (2004), hep-th/0403047.
- [2] R. Britto, F. Cachazo, and B. Feng, Nucl. Phys. **B715**, 499 (2005), hep-th/0412308.
- [3] Z. Bern, L. J. Dixon, D. C. Dunbar, and D. A. Kosower, Nucl. Phys. **B425**, 217 (1994), hep-ph/9403226.
- [4] R. Britto, F. Cachazo, and B. Feng, Nucl. Phys. **B725**, 275 (2005), hep-th/0412103.
- [5] G. Ossola, C. G. Papadopoulos, and R. Pittau, Nucl. Phys. **B763**, 147 (2007), hep-ph/0609007.
- [6] Y. Zhang, JHEP **1209**, 042 (2012), 1205.5707.
- [7] P. Mastrolia, E. Mirabella, G. Ossola, and T. Peraro, Phys.Lett. **B718**, 173 (2012), 1205.7087.
- [8] L. F. Alday and R. Roiban, Phys.Rept. **468**, 153 (2008), 0807.1889.
- [9] R. Britto, J.Phys.A **A44**, 454006 (2011), 34 pages. Invited review for a special issue of Journal of Physics A devoted to 'Scattering Amplitudes in Gauge Theories', 1012.4493.
- [10] J. M. Henn, J.Phys.A **A44**, 454011 (2011), 1103.1016.
- [11] Z. Bern and Y.-t. Huang, J.Phys.A **A44**, 454003 (2011), 1103.1869.
- [12] J. J. M. Carrasco and H. Johansson, J.Phys.A **A44**, 454004 (2011), 1103.3298.
- [13] L. J. Dixon, J.Phys.A **A44**, 454001 (2011), 1105.0771.
- [14] R. Ellis, Z. Kunszt, K. Melnikov, and G. Zanderighi (2011), 1105.4319.
- [15] H. Ita, J.Phys.A **A44**, 454005 (2011), 1109.6527.
- [16] G. Ossola, C. G. Papadopoulos, and R. Pittau, JHEP **0707**, 085 (2007), 0704.1271.
- [17] P. Mastrolia and G. Ossola, JHEP **1111**, 014 (2011), 1107.6041.
- [18] S. Badger, H. Frellesvig, and Y. Zhang, JHEP **1204**, 055 (2012), 1202.2019.
- [19] P. Mastrolia, E. Mirabella, G. Ossola, and T. Peraro, Phys.Lett. **B727**, 532 (2013), 1307.5832.
- [20] R. Pittau, JHEP **1211**, 151 (2012), 1208.5457.
- [21] A. M. Donati and R. Pittau, JHEP **1304**, 167 (2013), 1302.5668.
- [22] A. M. Donati and R. Pittau (2013), 1311.3551.
- [23] G. Mahlon, Phys.Rev. **D49**, 2197 (1994), hep-ph/9311213.
- [24] Z. Bern and A. G. Morgan, Nucl. Phys. **B467**, 479 (1996), hep-ph/9511336.
- [25] C. Anastasiou, R. Britto, B. Feng, Z. Kunszt, and P. Mastrolia, Phys.Lett. **B645**, 213 (2007), hep-ph/0609191.
- [26] C. Anastasiou, R. Britto, B. Feng, Z. Kunszt, and P. Mastrolia, JHEP **0703**, 111 (2007), hep-ph/0612277.
- [27] W. T. Giele, Z. Kunszt, and K. Melnikov, JHEP **0804**, 049 (2008), 0801.2237.
- [28] R. Ellis, W. T. Giele, Z. Kunszt, and K. Melnikov, Nucl.Phys. **B822**, 270 (2009), 0806.3467.
- [29] Z. Bern, L. J. Dixon, and D. A. Kosower, Phys.Rev.Lett. **70**, 2677 (1993), hep-ph/9302280.
- [30] Z. Bern, L. J. Dixon, D. C. Dunbar, and D. A. Kosower, Nucl.Phys. **B435**, 59 (1995), hep-ph/9409265.
- [31] G. Ossola, C. G. Papadopoulos, and R. Pittau, JHEP **0805**, 004 (2008), 0802.1876.
- [32] M. Garzelli, I. Malamos, and R. Pittau, JHEP **1101**, 029 (2011), 1009.4302.
- [33] K. Melnikov and M. Schulze, Nucl.Phys. **B840**, 129 (2010), 1004.3284.
- [34] S. Davies, Phys.Rev. **D84**, 094016 (2011), 1108.0398.
- [35] Z. Bern and D. A. Kosower, Nucl.Phys. **B379**, 451 (1992).
- [36] Z. Bern, A. De Freitas, L. J. Dixon, and H. Wong, Phys.Rev. **D66**, 085002 (2002), hep-ph/0202271.
- [37] C. Cheung and D. O'Connell, JHEP **0907**, 075 (2009), 0902.0981.
- [38] F. Cascioli, P. Maierhofer, and S. Pozzorini (2011), 1111.5206.
- [39] V. Hirschi, R. Frederix, S. Frixione, M. V. Garzelli, F. Maltoni, et al., JHEP **1105**, 044 (2011), 1103.0621.
- [40] S. Actis, A. Denner, L. Hofer, A. Scharf, and S. Uccirati, JHEP **1304**, 037 (2013), 1211.6316.
- [41] H. D. Vinod, *Hands-on matrix algebra using R. Active and motivated learning with applications*. (Hackensack, NJ: World Scientific, 2011), ISBN 978-981-4313-68-1.
- [42] R. Pittau, JHEP **1202**, 029 (2012), 1111.4965.
- [43] R. K. Ellis, W. J. Stirling, and B. R. Webber, *QCD and Collider Physics* (Cambridge University Press, 1996).
- [44] T. Hahn, Comput.Phys.Comm. **140**, 418 (2001), hep-ph/0012260.
- [45] T. Hahn and M. Perez-Victoria, Comput.Phys.Comm. **118**, 153 (1999), hep-ph/9807565.
- [46] S. Agrawal, T. Hahn, and E. Mirabella, J.Phys.Conf.Ser. **368**, 012054 (2012), 1112.0124.
- [47] B. Chokoufe Nejad, T. Hahn, J. N. Lang, and E. Mirabella (2013), 1310.0274.
- [48] Y. Katayama, K. Sawada, and S. Takagi, Progress of Theoretical Physics **5**, 14 (1950), URL <http://ptp.ipap.jp/link?PTP/5/14/>.
- [49] G. 't Hooft, Nucl.Phys. **B33**, 173 (1971).
- [50] D. Leiter and G. Szamosi, Lettere al Nuovo Cimento **5**, 814 (1972).
- [51] M. Trzetrzelewski (2011), 1101.3899.
- [52] U. Jentschura and B. Wundt, ISRN High Energy Phys. **2013**, 374612 (2013), 1205.0521.
- [53] G. Mahlon and S. J. Parke, Phys.Rev. **D58**, 054015 (1998), hep-ph/9803410.
- [54] F. Wilczek, Phys.Rev.Lett. **39**, 1304 (1977).
- [55] S. Dawson, Nucl.Phys. **B359**, 283 (1991).
- [56] S. D. Badger, JHEP **01**, 049 (2009), 0806.4600.
- [57] P. Mastrolia, Phys.Lett. **B644**, 272 (2007), hep-th/0611091.
- [58] D. Forde, Phys. Rev. **D75**, 125019 (2007), 0704.1835.
- [59] R. Britto, E. Buchbinder, F. Cachazo, and B. Feng, Phys.Rev. **D72**, 065012 (2005), hep-ph/0503132.
- [60] R. Britto, B. Feng, and P. Mastrolia, Phys.Rev. **D73**, 105004 (2006), hep-ph/0602178.
- [61] P. Mastrolia, Phys.Lett. **B678**, 246 (2009), 0905.2909.
- [62] W. B. Kilgore (2007), 0711.5015.
- [63] R. Britto and B. Feng, Phys.Lett. **B681**, 376 (2009), 0904.2766.
- [64] R. Britto and E. Mirabella, JHEP **1101**, 135 (2011), 1011.2344.
- [65] Z. Kunszt, A. Signer, and Z. Trocsanyi, Nucl.Phys. **B411**, 397 (1994), hep-ph/9305239.
- [66] Z. Bern, G. Chalmers, L. J. Dixon, and D. A. Kosower, Phys.Rev.Lett. **72**, 2134 (1994), hep-ph/9312333.
- [67] A. Brandhuber, S. McNamara, B. J. Spence, and G. Travaglini, JHEP **0510**, 011 (2005), hep-th/0506068.

- [68] L. J. Dixon (1996), hep-ph/9601359.
- [69] S. Badger, E. N. Glover, V. Khoze, and P. Svrcek, JHEP **0507**, 025 (2005), hep-th/0504159.
- [70] Z. Bern, L. J. Dixon, and D. A. Kosower, Nucl.Phys. **B437**, 259 (1995), hep-ph/9409393.
- [71] C. R. Schmidt, Phys.Lett. **B413**, 391 (1997), hep-ph/9707448.
- [72] A. van Hameren, JHEP **0907**, 088 (2009), 0905.1005.
- [73] G. Heinrich, G. Ossola, T. Reiter, and F. Tramontano, JHEP **1010**, 105 (2010), 1008.2441.
- [74] P. Mastrolia, G. Ossola, T. Reiter, and F. Tramontano, JHEP **1008**, 080 (2010), 1006.0710.
- [75] P. Mastrolia, E. Mirabella, and T. Peraro (2012), 1203.0291.
- [76] T. Peraro (2014), 1403.1229.
- [77] G. Cullen, N. Greiner, G. Heinrich, G. Luisoni, P. Mastrolia, et al. (2011), 1111.2034.
- [78] Z. Bern and G. Chalmers, Nucl.Phys. **B447**, 465 (1995), hep-ph/9503236.